Cell Metabolism
Short Article

NDUFA4 Is a Subunit of Complex IV of the Mammalian Electron Transport Chain

Eduardo Balsa,[1,2] Ricardo Marco,[1] Ester Perales-Clemente,[1] Radek Szklarczyk,[3] Enrique Calvo,[1] Manuel O. Landázuri,[2] and José Antonio Enríquez[1,4,*]
[1]Centro Nacional de Investigaciones Cardiovasculares Carlos III (CNIC), Madrid, 28029, Spain
[2]Servicio de Inmunología, Hospital Universitario de La Princesa, Universidad Autónoma de Madrid, Instituto de Investigación Sanitaria Princesa (IIS-IP), Madrid, 28006, Spain
[3]Centre for Molecular and Biomolecular Informatics, Nijmegen Centre for Molecular Life Sciences, Radboud University Medical Centre, PO Box 9101, 6500HB, Nijmegen, The Netherlands
[4]Departamento de Bioquímica y Biología Molecular y Celular, Facultad de Ciencias, Universidad de Zaragoza, 50013, Spain
*Correspondence: jaenriquez@cnic.es
http://dx.doi.org/10.1016/j.cmet.2012.07.015

SUMMARY

The oxidative phosphorylation system is one of the best-characterized metabolic pathways. In mammals, the protein components and X-ray structures are defined for all complexes except complex I. Here, we show that NDUFA4, formerly considered a constituent of NADH Dehydrogenase (CI), is instead a component of the cytochrome *c* oxidase (CIV). Deletion of NDUFA4 does not perturb CI. Rather, proteomic, genetic, evolutionary, and biochemical analyses reveal that NDUFA4 plays a role in CIV function and biogenesis. The change in the attribution of the NDUFA4 protein requires renaming of the gene and reconsideration of the structure of CIV. Furthermore, NDUFA4 should be considered a candidate gene for CIV rather than CI deficiencies in humans.

INTRODUCTION

The OXPHOS system is one of the better and more deeply characterized metabolic pathways (Saraste, 1999). It is composed of four respiratory complexes, called complex I (NADH-ubiquinone oxidoreductase), complex II (succinate:ubiquinone oxidoreductase), complex III (ubiquinol-cytochrome *c* reductase), and complex IV (cytochrome *c* oxidase); the electron carriers ubiquinone (UQ or CoQ) and cytochrome *c* (cyt c); and the H^+-ATP synthase (complex V). All the structural protein components of the mammalian OXPHOS system are thought to be known. Complex I is composed of 45 subunits, complex II of 4, complex III of 11, complex IV of 13, and complex V of 11 proteins. In addition, a large number of assembly factors continue to be described for all the complexes, and research into assembly pathways remains a highly active field (for review, see Fernández-Vizarra et al., 2009). The biochemical organization of the complexes is also well characterized, but several key issues remain to be deciphered: the organization of cofactors in CI is not yet fully solved (Roessler et al., 2010), the interaction of this complex with CoQ is not well established (Ohnishi et al., 2005; Shinzawa-Itoh et al., 2010), and the proton translocation mechanisms in CI and IV have not been fully determined (Xu and Voth, 2008). The X-ray structures of complex II (Sun et al., 2005), III (Iwata et al., 1998), and IV (Tsukihara et al., 1995, 1996) have been solved, as well as that of the F_1 domain and the membrane-extrinsic region of complex V (Abrahams et al., 1994; Rees et al., 2009) and the complex I structure of *E. coli* (Efremov et al., 2010; Efremov and Sazanov, 2011) and Yarrowia mitochondria (Hunte et al., 2010). However, the X-ray structures of complex I in higher eukaryotes and of F_O domain of ATP synthase remain unsolved (Fernández-Vizarra et al., 2009).

This formidable accumulation of information about the OXPHOS system has turned out to be insufficient to explain the phenotypic consequences of its dysfunction, and we are consequently confronted by an impressive lack of understanding about why, where, how, and when disease will manifest if the OXPHOS system is impaired. Moreover, research into specific diseases has revealed major shortcomings in the established models of electron transport chain organization (Acín-Pérez et al., 2004). Investigation of human OXPHOS diseases teaches us that our basic knowledge of the system is far from complete and that a description of the component elements, albeit exhaustive, does not provide a functional understanding of the system as a whole. Here, we demonstrate that even aspects that were considered to be fully established, such as the number and subunit composition of the respiratory complexes, need to be revised: we provide compelling evidence that NDUFA4, a protein considered to be a complex I structural subunit (Carroll et al., 2006), is in fact an essential structural protein of complex IV.

RESULTS

Different Comigrating Pattern of NDUFA4 in Blue Native Gels

To identify interactions between mitochondrial proteins that may be revealed by their comigration on native gels, we are implementing a systematic proteomic analysis of mitochondrial protein bands in blue-native gels (Figures 1A and 1B). Thus, we compared wild-type mouse cell lines with cells from mutants with specific loss of individual respiratory complexes (CI^{KO}, $CIII^{KO}$, or CIV^{KO}) or lacking mtDNA (ρ°-cells). To maximally preserve in vivo protein interactions, we solubilized mitochondrial membranes with digitonin (Acín-Pérez et al., 2008). Since the protein composition of the mammalian respiratory

complexes is well known (Carroll et al., 2006; Hirst et al., 2003; Iwata et al., 1998; Tsukihara et al., 1996), we examined them to determine the robustness of our approach and the level of sensitivity for highly hydrophobic mitochondrial inner membrane proteins. Our system detected 39 of the 45 CI proteins (Carroll et al., 2006; Hirst et al., 2003), 3 of the 4 CII proteins (Cecchini, 2003), 10 of the 11 CIII proteins (Iwata et al., 1998), and 8 of the 13 CIV proteins (Tsukihara et al., 1996) (Figure 1A). Our analysis also confirmed the comigration of complexes when assembled into different supercomplexes (I_2+III_2; I+III_2+IV_n; I+III_2; and III_2+ IV). Most of the proteins showed the expected distribution pattern on the BN gel, and knockout of one complex subunit not only almost abolished the detection of proteins of the same complex, but also deleted components of other complexes that associate in the same supercomplex (Figure 1A). Notably, although CI is degraded in the absence of CIII or IV, expression of CI proteins was better preserved in $CIII^{KO}$ cells, suggesting that CI is more unstable in the absence of CIV than in the absence of CIII (Figure 1A).

In departure from the expected behavior, we found NDUFA4 (unequivocally identified by three specific peptides; Figure S1), classically described as a CI subunit (Carroll et al., 2003; Hirst et al., 2003), in a distribution pattern consistent with components of CIV (Figure 1A). In control cells, NDUFA4 never occurred in positions where CI migrates alone; on the contrary, it always comigrated with CIV subunits, either at positions where CIV migrates alone, or assembled in supercomplex I+III_2+IV_n. Moreover, in CI^{KO} samples, where only four of the CI subunits are detected (NDUFS7, NDUFS3, NDUFA8, and ND1—comigrating in a previously described subcomplex [Vogel et al., 2007]), NDUFA4 was still present and comigrated with CIV. In contrast, in CIV^{KO} cells, NDUFA4 was deleted, together with all CIV proteins (Figure 1A). Moreover, in $CIII^{KO}$ cells, almost all CI subunits are detected as individual CI; but NDUFA4 again comigrated with CIV subunits. This proteomic analysis shows that NDUFA4 behaves like a CIV protein.

NDUFA4 Interacts with Proteins of Complex IV

To validate the proteomic analysis, we conducted immunoprecipitation experiments to determine whether NDUFA4 interacts directly with CIV. Endogenous NDUFA4 was specifically precipitated by antibodies targeting CIV subunits, but not by antibodies targeting CI (Figure 1C). Specific immunodetection analysis also confirmed comigration of NDUFA4 with CIV (Figure 1D), and resolving two-dimension gels showed NDUFA4 comigrating with CIV subunits (Figure 1E). Furthermore, in mouse cells lacking either ND4 or ND6, which showed a complete absence of CI when tested for several canonical proteins for this complex, NDUFA4 remained at the position of CIV (Figure 2A). In contrast, in mouse cells lacking COX10 ($COX10^{KO}$), which cannot fully assemble CIV, NDUFA4 comigrated with an immature form of CIV, and in human cells lacking COX2 ($COX2^{KO}$), which are similarly unable to form CIV, NDUFA4 was completely absent (Figure 2B). These results strongly indicate that NDUFA4 is a subunit of CIV and not CI. Furthermore, we notice that, contrary to what was found for mouse cultured cells (Diaz et al., 2006), human cells lacking CIV (see Figure S2 for a characterization of the $Cox2^{KO}$ cells) are still able to retain a significant amount of assembled CI (Figure 2C) that mainly interact with CIII. In these cells complex NDUFA4 is not detected. To ensure that CI was fully active despite the absence of NDUFA4 and CIV, we performed in-gel activity for NADH dehydrogenase (CI) or for CIV. Complex IV activity was detected in both wild-type and 80% mutant Cox2 cells, but not in 100% mutant Cox2 ones (Figure 2D). However, in-gel CI activity is easily appreciated in all tested cell lines regardless of whether they have CIV or not (Figure 2D). To determine if this NADH dehydrogenase activity was reflecting a true functional CI in vivo, we transformed $Cox2^{KO}$ cells with AOX (an alternative electron transport system present in lower eukaryotes, plants, and lower animals that can perform the overall oxidation of $CoQH_2$, instead of CIII and CIV, which are able to work in mammalian cells [Perales-Clemente et al., 2008]). The expression of AOX does not modify qualitatively the presence of CI or its in-gel activity detection (Figures 2C and 2D). It allows $Cox2^{KO}$ to respire to a robust rate and, this respiration being substantially sensitive to rotenone, a CI-specific inhibitor (Figure 2E). This demonstrates that NDUFA4 is not required to form a fully functional CI.

Targeting NDUFA4 Protein Disrupts Normal Levels of Complex IV

If NDUFA4 is a genuine CIV subunit, its downregulation is likely to affect CIV activity. To test this, we stably silenced NDUFA4 in HeLa cells and monitored the activity and stability of CI and CIV. Upon downregulation of NDUFA4, CIV levels were reduced, whereas CI and CIII showed no obvious change (Figure 3A). Two-dimensional western blot also revealed reduced levels of CIV, although no preassembled complexes were detected (Figure 3B). To confirm that the phenotype induced by NDUFA4 silencing was entirely due to the reduced expression of this protein, we performed rescue experiments, in which myc-tagged NDUFA4 was overexpressed in stably NDUFA4 interfered cells. To allow myc-NDUFA4 expression, the locus for the endogenous NDUFA4 interference was removed in the myc-NDUFA4. Exogenous NDUFA4 fully restored CIV levels (Figure 3C), confirming the role of these proteins in cytochrome *c* oxidase maintenance and function.

The protein expression changes were paralleled by changes in CIV activity, with a decrease in activity observed in shNDUFA4 HeLa cells (Figure 3D) that was restored by overexpression of myc-NDUFA4. These changes were not accompanied by significant alterations in CI activity (not shown). Culture in galactose medium, which forces cells to rely on OXPHOS-dependent generation of ATP, demonstrated that the reduced CIV activity in NDUFA4-interfered cells inhibited proliferation compared with nonsilenced counterparts (Figure 3E).

The Evolution of NDUFA4 Correlated with That of Complex IV

Previous evolutionary analyses of *NDUFA4* indicated its presence outside vertebrate evolutionary clade (Gabaldón et al., 2005), and more recently outside metazoa (Huynen et al., 2009), yet NDUFA4 has not been confirmed to be a genuine complex I subunit in fungi or plants (Cardol, 2011). Due to high sequence divergence rates to identify *NDUFA4* homologs in eukaryotic species, we used hidden Markov models, similar to approaches employed to establish new COX assembly factors (Szklarczyk et al., 2012). Using sensitive homology searches,

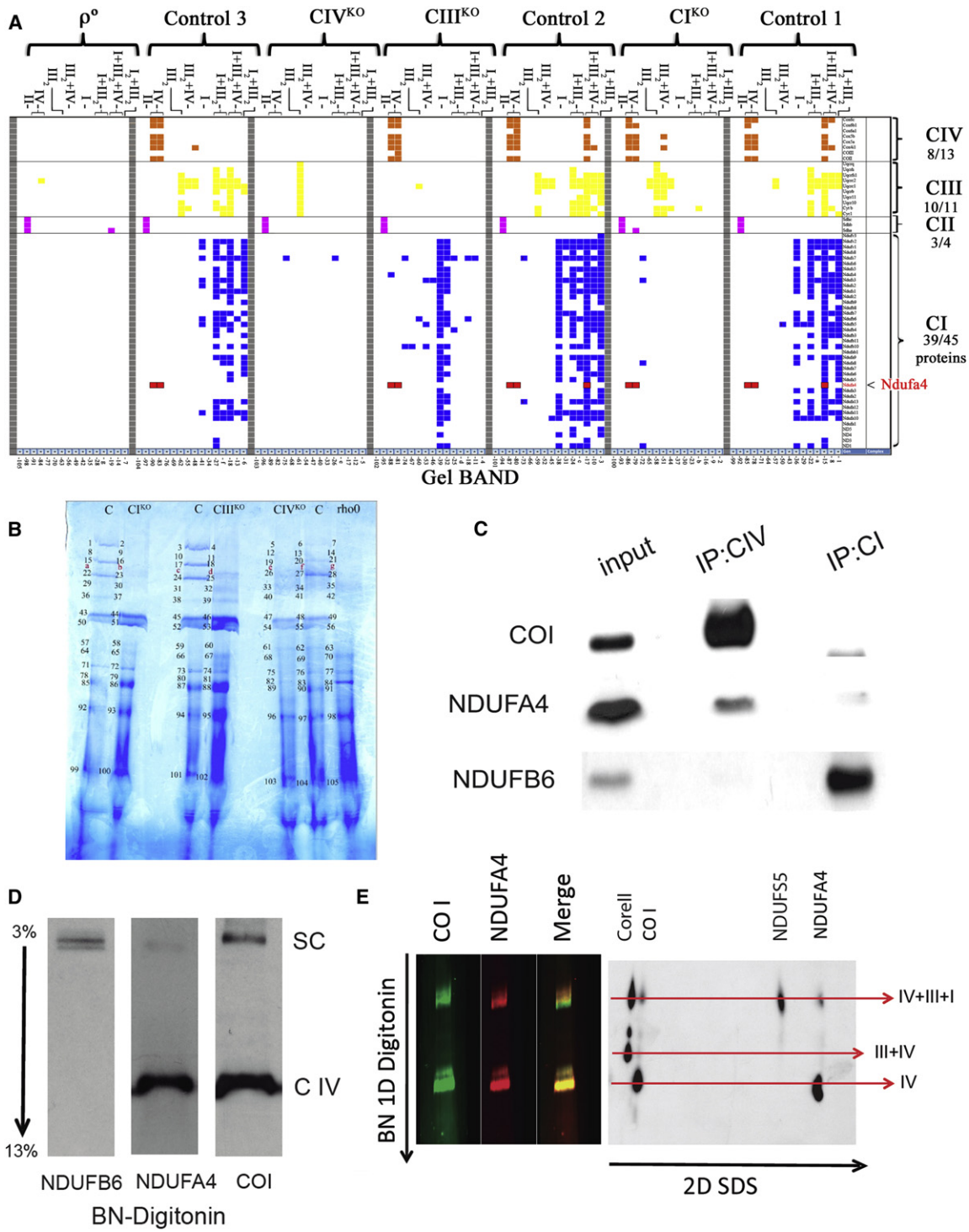

Figure 1. The NDUFA4 Protein Behaves as a Structural Component of Complex IV

(A) Scheme of retrieved peptides from MS/MS analysis of the gel slices cut from the gel shown in (B) (numbers under the graphic correspond to the gel slice number indicated in B). The position of the free complexes or supercomplexes is indicated on top for each line run on gel B and labeled as the indicated control or mutant cell line. In the scheme can be followed the distinct behavior of mitochondrial electron transport complex proteins (indicated at the right side, NDUFA4 is highlighted). Different colors identify components of individual complexes (complex I, blue; complex II, pink; complex III, yellow; complex IV, orange; NDUFA4 is shown in red).

(B) Representative Coomassie-stained blue native gel from which the bands were excised for the proteomic analysis summarized in (A). The gel was loaded with extracts from wild-type cells and cell lines depleted for specific mitochondrial electron transport complexes: control, wild-type cells; CI^{KO}, cells lacking complex I; $CIII^{KO}$, cells lacking complex III; CIV^{KO}, cells lacking complex IV; ρ°, mtDNA-less cells lacking complexes I, III, and IV.

we discovered that *NDUFA4* homologs' presence-absence patterns are not congruent with evolution of complex I as previously thought. Analysis of *NDUFA4* presence-absence patterns in fungi (Figure 4A) reveals the existence of the NDUFA4 gene in all OXPHOS-encoding species. We identified *NDUFA4* in *Saccharomyces cerevisiae* and other *Saccharomycetaceae* that have lost CI (Figure 4A). The yeast's protein, encoded by a gene of unknown function, YPR010C-A, shares common features with the human NDUFA4, such as short length (81 amino acids in human and 72 in yeast) and the N-terminal transmembrane region (Figure 4B). While little is known about the gene's function in yeast, the protein has recently been copurified together with supercomplex III/IV from digitonin-solubilized mitochondria (Vukotic et al., 2012). The YPR010C-A protein sequence in *S. cerevisiae* is not divergent from CI-containing *NDUFA4* in a related fungus, *Debaryomyces hansenii*, indicating that the CI loss in the ancestor of yeast did not significantly alter the rate of sequence evolution of the gene. A high sequence divergence due to a relaxed evolutionary pressure would be expected if the gene's primary role in fungi related to CI. Also in the fission yeast *Schizosaccharomyces pombe*, species that lost CI independently from the budding yeast (Figure 4A), we identify the *NDUFA4* homolog encoded by SPBC3H7.08c gene (Figure 4B). Outside fungi, the gene can be found in CI-lacking apicomplexans, including the malaria parasite *Plasmodium falciparum* (Figure 4B). Worth noting is the loss of *NDUFA4* in *Blastocystis hominis*, a species that encodes CI in its genome, but lacks complexes III, IV, and V. Taken together, the analysis of *NDUFA4* gene evolution argues against the gene's involvement in CI and supports the protein's role in CIV function.

DISCUSSION

Our findings are in clear conflict with the published crystal structures for cytochrome *c* oxidase. These revealed 13 distinct protein subunits, five phosphatidyl ethanolamines, three phosphatidyl glycerols and two cholates, two heme A molecules, three copper II ions, one magnesium ion, and one zinc ion, but no trace of NDUFA4. We hypothesized that NDUFA4 subunit might be lost during the purification of CIV in order to generate crystals. To obtain a high-quality crystal, samples are stringently purified using a wide range of detergents. One of the standard detergents used to purify CIV for crystallization purposes is n-dodecyl β-D-maltoside (DDM). We found that concentrations of DDM above 1.5% disrupt the interaction of NDUFA4 with CIV without affecting the remaining proteins (Figure S3). We therefore propose that this is the underlying cause for the failure of crystallization studies to detect NDUFA4 in CIV.

NDUFA4 was originally cataloged by Walker and coworkers as an accessory subunit of the mitochondrial membrane respiratory chain NADH dehydrogenase, or CI (Carroll et al., 2002, 2003, 2006; Hirst et al., 2003); however, the authors found several contradictory lines of evidence that made them doubt whether NDUFA4 was a genuine CI subunit (Hirst et al., 2003). In fact, NDUFA4 was not detected in all CI preparations and, more importantly, its presence correlated with contamination by the cytochrome *c* oxidase subunit VIB (Hirst et al., 2003). It may therefore be that the absence of NDUFA4 from CI preparations depends on detergent-mediated removal of cardiolipin, as occurs with other cytochrome *c* oxidase components, such as subunit VIB (Sedlák and Robinson, 1999). It is likely that, despite these warning signs, the established subunit composition of the other respiratory complexes based on their crystallization led to the acceptance of NDUFA4 as a CI subunit (Hirst et al., 2003). More recent evidence indicates that the expression pattern of NDUFA4 diverges notably from other CI nDNA-encoded subunits, leading to speculation that NDUFA4 may have other roles in addition to being a subunit of CI (Garbian et al., 2010). The full significance of these doubts and discrepancies is made clear in the light of our observations.

The change in the assignation of NDUFA4 from CI to CIV has important and wide implications. First, it may require redefinition of the structure of CIV. Second, it may now be necessary to consider NDUFA4 as a candidate gene for CIV deficiencies in humans, rather than for CI deficiencies. And third, it calls the attention to protocols for protein crystallization, especially from membrane protein complexes, because some proteins can be washed out during the multistep detergent-based purification of the crystals.

EXPERIMENTAL PROCEDURES

Cell Lines and Media

Mouse fibroblasts (wild-type, $COX10^{KO}$, $ND4^{KO}$, and $ND6^{KO}$), human fibroblasts (wild-type and $COX2^{KO}$), and HeLa cells were cultured in DMEM containing 10% heat-inactivated fetal bovine serum (FBS). All media were supplemented with 100 IU/ml penicillin and 100 μg/ml streptomycin. $COX10^{KO}$ and $COX2^{KO}$ fibroblasts were also supplemented with 50 mg/ml uridine. MtDNA-less mouse cells (ρ°L929) were grown in DMEM supplemented with 5% FBS, 50 mg/ml uridine, and 1 mM pyruvate (ρ° medium) and in the presence of 250 mg/ml of geneticin (G418). Medium for cells stably knocked down for NDUFA4 was supplemented with 1 μg/ml puromycin. Cells were maintained in 5% CO_2/95% air at 37°C.

shRNA and Expression Vectors

HeLa cells were stably transfected with one of two shRNA targeting sequences for NDUFA4 (sh.38 and sh.41). Specific lentivirus particles were purchased from Dharmacon. Empty vector or PCMV containing the NDUFA4 open reading frame were from OriGene and were used to transfect control HeLa cells and cells knocked down with sh.38 and sh.41 shRNAs.

Isolation of Mitochondria

Mitochondria were isolated from cultured cell lines according to Fernández-Vizarra et al., 2002, with some modifications. The following detergents were used for extracting mitochondrial membrane proteins: n-dodecyl β-D-maltoside (DDM) at 0.5%, 1%, or 3%; digitonin (DIG) at 4 g/g.

Blue Native Gel Electrophoresis and Western Blot Analysis

Mitochondrial membrane proteins (100–150 μg) were applied and run on 3%–13% first-dimension gradient BN gels as described elsewhere

(C) Isolated mitochondria from HeLa cells were solubilized with 1% DDM and immunoprecipitated with specific antibodies against either CIV or CI. COI and NDUFA4 both coimmunoprecipitate with CIV, whereas NDUFB6 coimmunoprecipitates with CI exclusively.
(D and E) Isolated mitochondria from HeLa cells were digitonized and resolved by one-dimensional BNGE (D) or by BNGE followed by a second dimension of SDS-PAGE (E). After electrophoresis, membranes were probed with antibodies specific for CI (NDUFB6 and NDUFS5), CIII (Core II), CIV (COI), and NDUFA4.

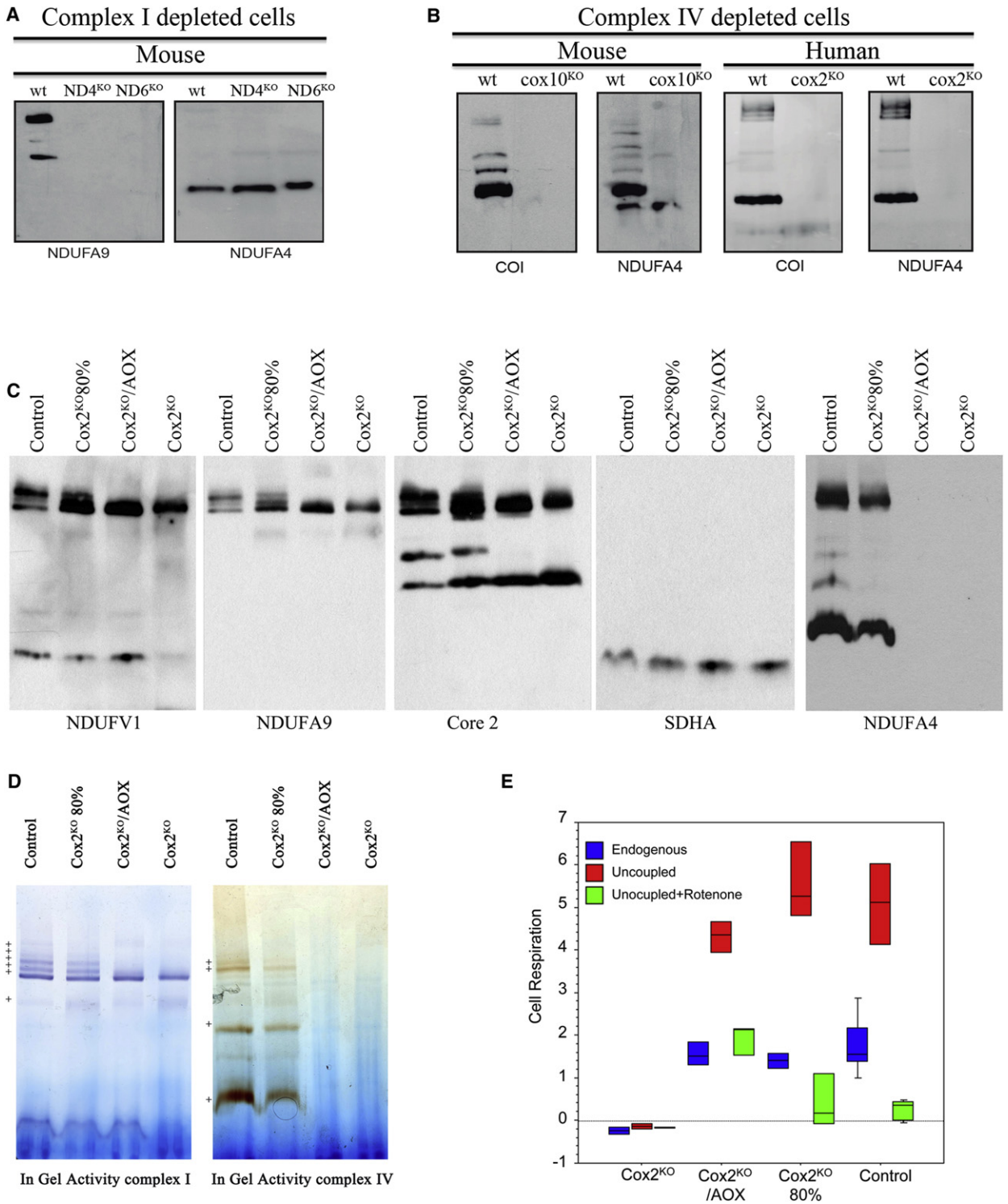

Figure 2. BNGE Analysis in Mutant Fibroblast Lines Lacking Either Complex IV or Complex I

(A) CI depleted cells: mouse fibroblasts lacking ND4 and ND6.

(B) CIV depleted cells: mouse fibroblasts lacking COX10 and human fibroblasts lacking COX2.

(C) Human cells lacking COX2 and expressing or not AOX or with 80% of the mutant Cox2 gene probed against complex I (NDUFV1, NDUFA9), complex III (Core2), complex II (SDHA), and NDUFA4. Western blots were probed with antibodies against the proteins indicated beneath the blots in (A)–(C).

(D) In-gel activity of a paralleled run gels to that of (C) above.

(E) Box plot showing oxygen consumption by the indicated intact cells under coupled or uncoupled conditions (by CCCP) and effect of CI activity inhibition by rotenone. Box plot represents data distribution by different quartile.

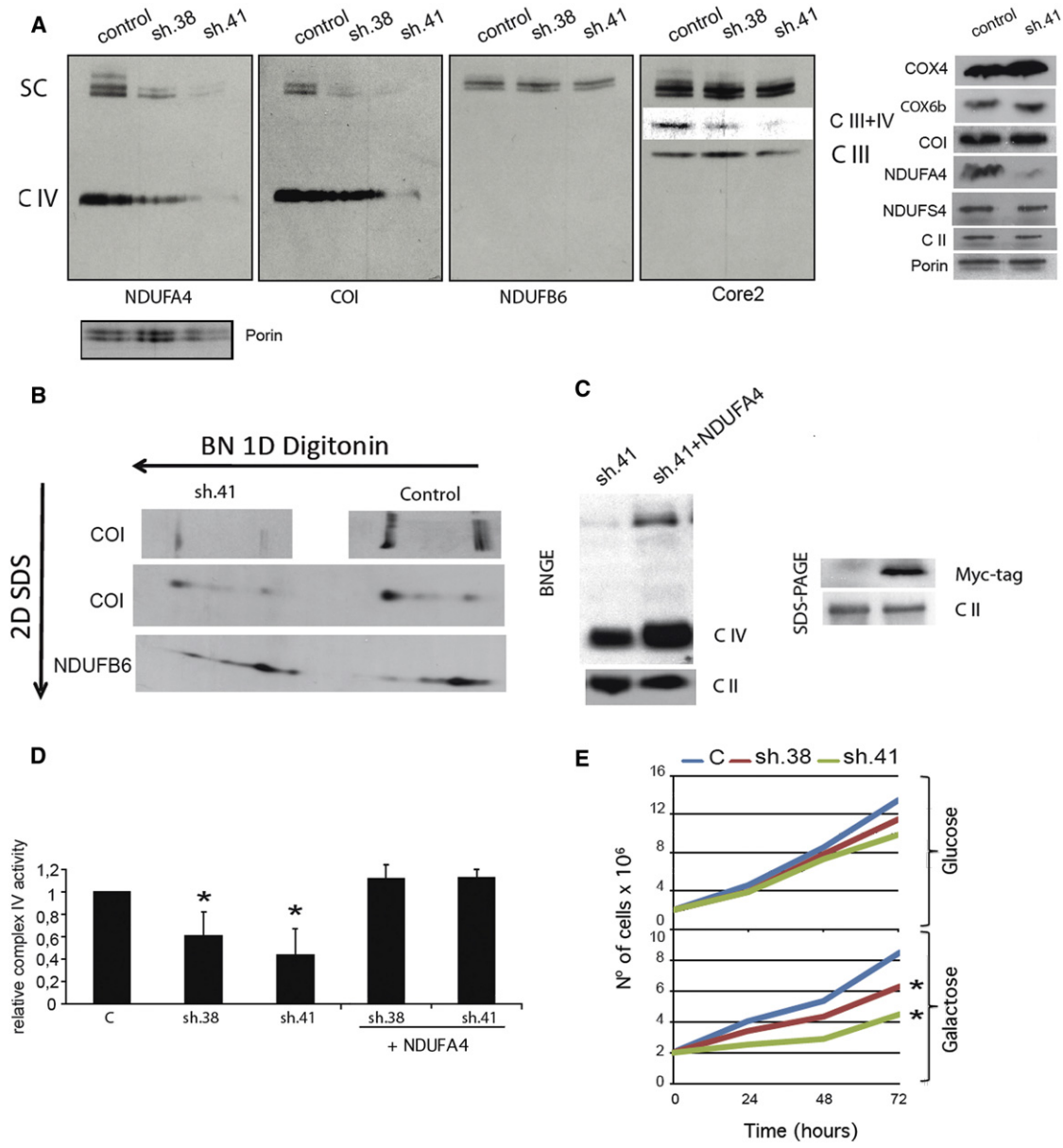

Figure 3. Complex IV Is Impaired in the Absence of NDUFA4

(A–D) NDUFA4 was stably knocked down in HeLa cells using two different NDUDA4-targeting shRNA sequences (sh.38 and sh.41). (A) Left: BNGE analysis of digitonin-isolated mitochondria, followed by western blot with antibodies against the indicated protein. Notice that on the core 2 blot, the band for CIII + CIV is a different exposure to better show that the supercomplex III + IV is also lost by the interference of NDUFA4. SC: supercomplexes. Right: western blots of SDS-PAGE analysis of control and sh.41 cells. Porin was used as a loading control. (B) Western blots of 2D electrophoresis gels (BNGE followed by SDS-PAGE) of control and sh.41 cells; membranes were probed with antibodies against the indicated proteins. (C) Left: BNGE analysis revealing restoration of CIV levels in sh.41 cells after exogenous overexpression of myc-tagged NDUFA4. Right: SDS-PAGE showing expression levels of myc-NDUFA4; CII was used as a loading control. (D) CIV activity relative to citrate synthase was measured spectrophotometrically in isolated mitochondria from control cells. Error bars indicate standard deviation of the mean. (C), NDUFA4-silenced cells (sh.38 and sh.41), and NDUFA4-silenced cells expressing myc-NDUFA4 (+NDUFA4) (E). Growth curves of control and NDUFA4-silenced HeLa cells culture in medium containing glucose or galactose. *$p < 0.05$ compared with control (Student's t test).

(Fernández-Vizarra et al., 2002). For 2D analysis, the first-dimension lane was excised from the gel, incubated for 1 hr at room temperature in 1% SDS and 1% β-mercaptoethanol, and run on a 16.5% second-dimension denaturing (SDS-PAGE) gel. After electrophoresis, the complexes were electroblotted onto PVDF membranes and sequentially probed with specific antibodies against CI (anti-NDUFB6, NDUFS5, NDUFS4, and NDUFA9), CIII (anti-core2), CIV (anti-COI), and CII (70 kDa subunit). All antibodies were from Molecular Probes. NDUFA4 antibody was purchased in Bioworld.

Protein Identification by Liquid Chromatography Coupled to Tandem Mass Spectrometry

Gel pieces from blue native gels containing the protein bands of interest were excised. After reduction with DTT (10 mM) and alkylation of Cys groups with

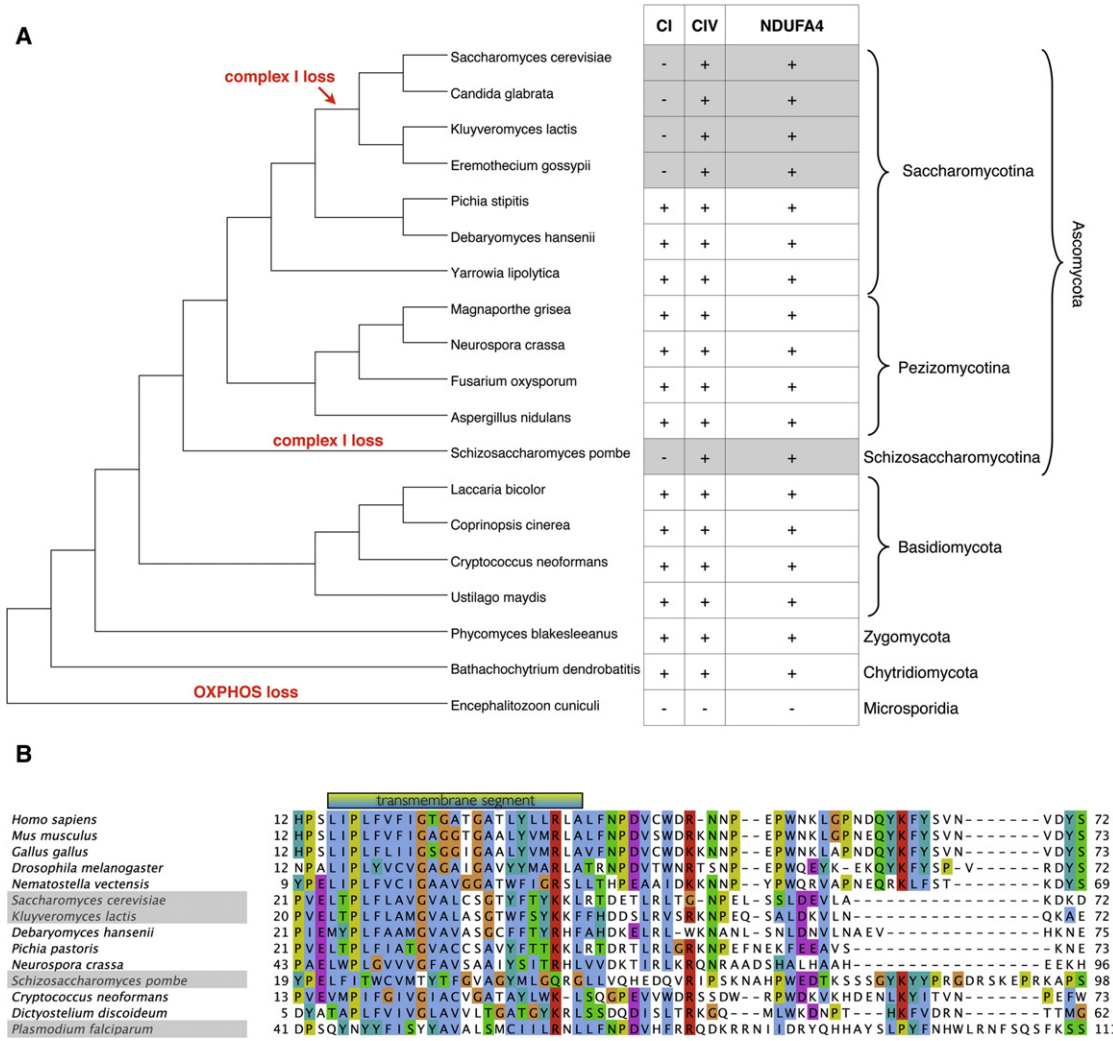

Figure 4. Sequence Evolution of NDUFA4 in Eukaryotes

(A) The analysis of NDUFA4 presence-absence patterns in fungi reveals that the NDUFA4 protein does not follow the evolutionary pattern of CI losses. Fungal species tree (Lavín et al., 2008) with indicated independent losses of respiratory chain complexes is shown. The isolated CI losses do not lead to the loss of NDUFA4, as would be expected if NDUFA4 was a CI subunit. CI, IV, and NDUFA4 presence patterns are marked in the table. Instances where CI is missing, but NDUFA4 is preserved, are marked gray.

(B) Multiple alignment of the conserved region of NDUFA4 in eukaryotes. Species without CI are marked gray. The transmembrane region (after TMHMM [Krogh et al., 2001]) that is common to all sequences is shown above the alignment. The alignment was prepared using Clustal-W with default parameters (Thompson et al., 1994). Sequence identifiers are listed in Table S1.

iodoacetamide (50 mM), modified porcine trypsin (Promega) was added at a final mass ratio of 1:50 (trypsin-protein). Digestion proceeded overnight at 37°C, after which samples were vacuum-dried and dissolved in 1% acetic acid.

To identify proteins, the resulting tryptic peptide mixtures were analyzed by nanoliquid chromatography coupled to mass spectrometry. Peptides were injected onto a C-18 reversed phase (RP) nanocolumn (100 μm I.D. and 15 cm, Mediterranea Sea, Teknokroma) and analyzed on a continuous acetonitrile gradient consisting of 0%–43% B for 90 min and 50%–90% B for 1 min (B = 95% acetonitrile, 0.5% acetic acid). Peptides were eluted from the RP nanocolumn at a flow rate of ~300 nl/min to an emitter nanospray needle for real-time ionization and peptide fragmentation on an LTQ-Orbitrap mass spectrometer (Thermo Fisher, San Jose, CA). An enhanced FT-resolution spectrum (resolution = 6,000) and the MS/MS spectra of the five most-intense parent ions were analyzed during the chromatographic run (130 min). Dynamic exclusion was set at 0.5 min.

For protein identification, tandem mass spectra were extracted and charge-state deconvoluted with Proteome Discoverer 1.2.0.207 (Thermo Fisher Scientific). All MS/MS samples were analyzed by SEQUEST (Thermo Fisher Scientific, version 1.0.43.2), MASCOT (Matrixscience, version 2.1) and X! Tandem (The GPM, http://thegpm.org; version 2007.01.01.1). Search engines were set up to search MSIPI_mouse_3.67.fasta (1.0, 56,687 entries). All searches were performed assuming complete trypsin digestion. Two mixed cleavages were allowed, and errors of 15 ppm or 0.8 Da were set for full MS and MS/MS spectra searches, respectively. Oxidation of M, phosphorylation of S or T, and deamidation of Q or N were selected as dynamic modifications. All identifications were made by Decoy database search for FDR analysis. Scaffold (version Scaffold_3_00_03, Proteome Software Inc., Portland, OR) was used to validate MS/MS peptide and protein identifications. Protein probabilities were assigned by the Protein Prophet algorithm. Proteins that contained similar peptides and could not be differentiated based on MS/MS analysis alone were grouped to satisfy the principles of parsimony.

Immunocapture of Mitochondrial Complex I and IV OXPHOS Complexes

Mitochondrial CI or CIV was immunocaptured from isolated mitochondria using the CI and CIV immunoprecipitation kit (Abcam) according to the manufacturer's instructions.

Activities of Complex I and IV

CI and CIV activities were measured spectrophotometrically in mitochondrial fractions (2–5 mg protein) as described (Hofhaus et al., 1996). Both activities were expressed relative to citrate synthase activity.

Proliferation Analysis

Control, sh.38, and sh.41 HeLa cells were plated at 2×10^5 per 10 cm dish in DMEM containing either glucose or galactose. At indicated times the cells were trypsinized and the viable cells were counted.

Analysis of Genomic Presence-Absence Patterns

Homologs of the human NDUFA4 gene (Swissprot id: O00483) were retrieved with three iterations of PSI-BLAST with default parameters (Altschul et al., 1997). An alignment was build with default parameters of Clustal-W (Thompson et al., 1994) and profile and a profile-based hidden Markov model (HMM) of NDUFA4 gene were created based on the conserved part of the multiple alignment with HMMER 3.0 (http://hmmer.org) and HHSearch 1.5 (PMID: 15531603). The HMMs ware used to retrieve homologs in eukaryotes. Only statistically significant reciprocal-best hits highly indicative of orthology (Szklarczyk et al., 2012) were taken into account. The absence of the gene in *B. hominis* was confirmed at the genome level (by searching species' DNA, without prior knowledge of its gene compendium) to account for possibility of gene missing from *B. hominis* genome annotation.

Statistical Analysis

The data are presented as the means ± standard deviation of the mean of at least three independent experiments. Statistical significance ($^*p < 0.05$) was assessed by Student's t test.

SUPPLEMENTAL INFORMATION

Supplemental Information includes three figures and one table and can be found with this article online at http://dx.doi.org/10.1016/j.cmet.2012.07.015.

ACKNOWLEDGMENTS

We thank Dr. Ugalde for providing the $COXII^{KO}$ primary fibroblasts; Dr. Concepción Jimenez, Marta Roche, and Andres Gonzalez for technical assistance; and Dr. Simon Bartlett (CNIC) for English editing. This study was supported by grants from the MEC (SAF2009-08007 and CSD2007-00020) and CAM (S2010/BMD-2402). The CNIC is supported by the MEC and the Pro-CNIC Foundation. R.S. is supported by the CSBB, The Netherlands. E.B., E.P.-C., R.M., R.S., and E.C. performed experimental work and analyses. E.B., M.O.L., and J.A.E. designed the research. J.A.E. directed the work. E.B. and J.A.E. wrote the manuscript.

Received: April 16, 2012
Revised: June 18, 2012
Accepted: July 26, 2012
Published online: August 16, 2012

REFERENCES

Abrahams, J.P., Leslie, A.G., Lutter, R., and Walker, J.E. (1994). Structure at 2.8 A resolution of F1-ATPase from bovine heart mitochondria. Nature *370*, 621–628.

Acín-Pérez, R., Bayona-Bafaluy, M.P., Fernández-Silva, P., Moreno-Loshuertos, R., Pérez-Martos, A., Bruno, C., Moraes, C.T., and Enríquez, J.A. (2004). Respiratory complex III is required to maintain complex I in mammalian mitochondria. Mol. Cell *13*, 805–815.

Acín-Pérez, R., Fernández-Silva, P., Peleato, M.L., Pérez-Martos, A., and Enriquez, J.A. (2008). Respiratory active mitochondrial supercomplexes. Mol. Cell *32*, 529–539.

Altschul, S.F., Madden, T.L., Schäffer, A.A., Zhang, J., Zhang, Z., Miller, W., and Lipman, D.J. (1997). Gapped BLAST and PSI-BLAST: a new generation of protein database search programs. Nucleic Acids Res. *25*, 3389–3402.

Cardol, P. (2011). Mitochondrial NADH:ubiquinone oxidoreductase (complex I) in eukaryotes: a highly conserved subunit composition highlighted by mining of protein databases. Biochim. Biophys. Acta *1807*, 1390–1397.

Carroll, J., Shannon, R.J., Fearnley, I.M., Walker, J.E., and Hirst, J. (2002). Definition of the nuclear encoded protein composition of bovine heart mitochondrial complex I. Identification of two new subunits. J. Biol. Chem. *277*, 50311–50317.

Carroll, J., Fearnley, I.M., Shannon, R.J., Hirst, J., and Walker, J.E. (2003). Analysis of the subunit composition of complex I from bovine heart mitochondria. Mol. Cell. Proteomics *2*, 117–126.

Carroll, J., Fearnley, I.M., Skehel, J.M., Shannon, R.J., Hirst, J., and Walker, J.E. (2006). Bovine complex I is a complex of 45 different subunits. J. Biol. Chem. *281*, 32724–32727.

Cecchini, G. (2003). Function and structure of complex II of the respiratory chain. Annu. Rev. Biochem. *72*, 77–109.

Diaz, F., Fukui, H., Garcia, S., and Moraes, C.T. (2006). Cytochrome c oxidase is required for the assembly/stability of respiratory complex I in mouse fibroblasts. Mol. Cell. Biol. *26*, 4872–4881.

Efremov, R.G., and Sazanov, L.A. (2011). Structure of the membrane domain of respiratory complex I. Nature *476*, 414–420.

Efremov, R.G., Baradaran, R., and Sazanov, L.A. (2010). The architecture of respiratory complex I. Nature *465*, 441–445.

Fernández-Vizarra, E., López-Pérez, M.J., and Enriquez, J.A. (2002). Isolation of biogenetically competent mitochondria from mammalian tissues and cultured cells. Methods *26*, 292–297.

Fernández-Vizarra, E., Tiranti, V., and Zeviani, M. (2009). Assembly of the oxidative phosphorylation system in humans: what we have learned by studying its defects. Biochim. Biophys. Acta *1793*, 200–211.

Gabaldón, T., Rainey, D., and Huynen, M.A. (2005). Tracing the evolution of a large protein complex in the eukaryotes, NADH:ubiquinone oxidoreductase (Complex I). J. Mol. Biol. *348*, 857–870.

Garbian, Y., Ovadia, O., Dadon, S., and Mishmar, D. (2010). Gene expression patterns of oxidative phosphorylation complex I subunits are organized in clusters. PLoS ONE *5*, e9985.

Hirst, J., Carroll, J., Fearnley, I.M., Shannon, R.J., and Walker, J.E. (2003). The nuclear encoded subunits of complex I from bovine heart mitochondria. Biochim. Biophys. Acta *1604*, 135–150.

Hofhaus, G., Shakeley, R.M., and Attardi, G. (1996). Use of polarography to detect respiration defects in cell cultures. Methods Enzymol. *264*, 476–483.

Hunte, C., Zickermann, V., and Brandt, U. (2010). Functional modules and structural basis of conformational coupling in mitochondrial complex I. Science *329*, 448–451.

Huynen, M.A., de Hollander, M., and Szklarczyk, R. (2009). Mitochondrial proteome evolution and genetic disease. Biochim. Biophys. Acta *1792*, 1122–1129.

Iwata, S., Lee, J.W., Okada, K., Lee, J.K., Iwata, M., Rasmussen, B., Link, T.A., Ramaswamy, S., and Jap, B.K. (1998). Complete structure of the 11-subunit bovine mitochondrial cytochrome bc1 complex. Science *281*, 64–71.

Krogh, A., Larsson, B., von Heijne, G., and Sonnhammer, E.L. (2001). Predicting transmembrane protein topology with a hidden Markov model: application to complete genomes. J. Mol. Biol. *305*, 567–580.

Lavín, J.L., Oguiza, J.A., Ramírez, L., and Pisabarro, A.G. (2008). Comparative genomics of the oxidative phosphorylation system in fungi. Fungal Genet. Biol. *45*, 1248–1256.

Ohnishi, T., Johnson, J.E., Jr., Yano, T., Lobrutto, R., and Widger, W.R. (2005). Thermodynamic and EPR studies of slowly relaxing ubisemiquinone species in the isolated bovine heart complex I. FEBS Lett. *579*, 500–506.

Perales-Clemente, E., Bayona-Bafaluy, M.P., Pérez-Martos, A., Barrientos, A., Fernández-Silva, P., and Enriquez, J.A. (2008). Restoration of electron transport without proton pumping in mammalian mitochondria. Proc. Natl. Acad. Sci. USA *105*, 18735–18739.

Rees, D.M., Leslie, A.G., and Walker, J.E. (2009). The structure of the membrane extrinsic region of bovine ATP synthase. Proc. Natl. Acad. Sci. USA *106*, 21597–21601.

Roessler, M.M., King, M.S., Robinson, A.J., Armstrong, F.A., Harmer, J., and Hirst, J. (2010). Direct assignment of EPR spectra to structurally defined iron-sulfur clusters in complex I by double electron-electron resonance. Proc. Natl. Acad. Sci. USA *107*, 1930–1935.

Saraste, M. (1999). Oxidative phosphorylation at the fin de siècle. Science *283*, 1488–1493.

Sedlák, E., and Robinson, N.C. (1999). Phospholipase A(2) digestion of cardiolipin bound to bovine cytochrome c oxidase alters both activity and quaternary structure. Biochemistry *38*, 14966–14972.

Shinzawa-Itoh, K., Seiyama, J., Terada, H., Nakatsubo, R., Naoki, K., Nakashima, Y., and Yoshikawa, S. (2010). Bovine heart NADH-ubiquinone oxidoreductase contains one molecule of ubiquinone with ten isoprene units as one of the cofactors. Biochemistry *49*, 487–492.

Sun, F., Huo, X., Zhai, Y., Wang, A., Xu, J., Su, D., Bartlam, M., and Rao, Z. (2005). Crystal structure of mitochondrial respiratory membrane protein complex II. Cell *121*, 1043–1057.

Szklarczyk, R., Wanschers, B.F., Cuypers, T.D., Esseling, J.J., Riemersma, M., van den Brand, M.A., Gloerich, J., Lasonder, E., van den Heuvel, L.P., Nijtmans, L.G., and Huynen, M.A. (2012). Iterative orthology prediction uncovers new mitochondrial proteins and identifies C12orf62 as the human ortholog of COX14, a protein involved in the assembly of cytochrome c oxidase. Genome Biol. *13*, R12.

Thompson, J.D., Higgins, D.G., and Gibson, T.J. (1994). CLUSTAL W: improving the sensitivity of progressive multiple sequence alignment through sequence weighting, position-specific gap penalties and weight matrix choice. Nucleic Acids Res. *22*, 4673–4680.

Tsukihara, T., Aoyama, H., Yamashita, E., Tomizaki, T., Yamaguchi, H., Shinzawa-Itoh, K., Nakashima, R., Yaono, R., and Yoshikawa, S. (1995). Structures of metal sites of oxidized bovine heart cytochrome c oxidase at 2.8 A. Science *269*, 1069–1074.

Tsukihara, T., Aoyama, H., Yamashita, E., Tomizaki, T., Yamaguchi, H., Shinzawa-Itoh, K., Nakashima, R., Yaono, R., and Yoshikawa, S. (1996). The whole structure of the 13-subunit oxidized cytochrome c oxidase at 2.8 A. Science *272*, 1136–1144.

Vogel, R.O., Smeitink, J.A., and Nijtmans, L.G. (2007). Human mitochondrial complex I assembly: a dynamic and versatile process. Biochim. Biophys. Acta *1767*, 1215–1227.

Vukotic, M., Oeljeklaus, S., Wiese, S., Vögtle, F.N., Meisinger, C., Meyer, H.E., Zieseniss, A., Katschinski, D.M., Jans, D.C., Jakobs, S., et al. (2012). Rcf1 mediates cytochrome oxidase assembly and respirasome formation, revealing heterogeneity of the enzyme complex. Cell Metab. *15*, 336–347.

Xu, J., and Voth, G.A. (2008). Redox-coupled proton pumping in cytochrome c oxidase: further insights from computer simulation. Biochim. Biophys. Acta *1777*, 196–201.